Journal of Hazardous Materials 498 (2025) 139875

Contents lists available at ScienceDirect

Journal of Hazardous Materials

journal homepage: www.elsevier.com/locate/jhazmat

Efficient removal of microplastic particles from wastewater through formation of heteroagglomerates during the activated sludge process

Guillaume Crosset-Perrotin [a], Mark Wiesner [b], Michael Sander [c], Thomas D. Bucheli [d], Eberhard Morgenroth [a,e], Ralf Kaegi [a,*]

[a] Eawag, Swiss Federal Institute of Aquatic Science and Technology, Duebendorf 8600, Switzerland
[b] Department of civil and environmental engineering, Duke University, Durham, NC 27708, United States
[c] ETH Zürich, Institute of Biogeochemistry and Pollutant Dynamics, Zürich 8092, Switzerland
[d] Agroscope, Environmental Analytics, Zürich 8046, Switzerland
[e] ETH Zürich, Institute of Environmental Engineering, Zürich 8093, Switzerland

HIGHLIGHTS

- More than 90 % of all microplastics (MP) variants accumulate in activated sludge.
- Formation of heteroagglomerates drive MP removal.
- Heteroagglomerates formed by differential sedimentation is more important than fluid shear.
- Relative affinities between MPs and sludge flocs are similar for most MP variants.
- MP concentrations in activated sludge inform about MP contents in effluent water.

GRAPHICAL ABSTRACT

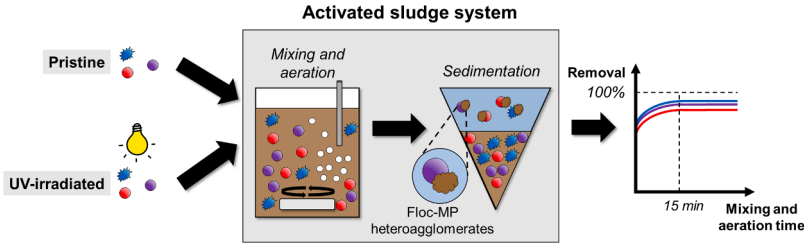

ARTICLE INFO

Keywords:
Microplastics
Heteroagglomeration
Activated sludge
Removal
Kinetic
Quality assurance / quality control
Aging

ABSTRACT

Microplastic particles (MPs) are efficiently transferred from wastewater to sludge during wastewater treatment, but it remains unclear to what extent the physical-chemical properties (e.g., polymer type, shape, size) of the MPs affect their incorporation into heteroagglomerates. To assess the latter, different variants of MPs were individually spiked to activated sludge, which was aerated and mixed for durations between 0 and 120 min, followed by 30 min of sedimentation. In experiments with no aeration/mixing, already 70 – 80 % of all MP variants were found in the sedimented sludge. Including 120 min of aeration/mixing resulted in an additional accumulation of 15 – 20 % of the MPs in the sedimented sludge, with steady state conditions being reached after less than 15 min aeration/mixing. Overall, more than 90 % of all MP variants were accumulated in the sedimented sludge and up to 10 % remained in the supernatant. The similar relative affinities of spiked MP variants to sludge flocs derived from time resolved experiments (increasing aeration/mixing time followed by 30 min sedimentation time) agree with the similar behavior of all MPs during the activated sludge process. Images of flocs collected at the end of the experiments showed that MPs were dominantly associated with flocs. The formation of heteroagglomerates was likely favored by the close-to-neutral zeta potential of the MPs in filtered wastewater, suggesting that van der Waals forces control heteroagglomerate formation. Taken together, these results indicate that the removal of MPs

* Correspondence to: Eawag, Swiss Federal Institute of Aquatic Science and Technology, 133 Ueberlandstrasse, Duebendorf 8600, Switzerland.
E-mail address: ralf.kaegi@eawag.ch (R. Kaegi).

https://doi.org/10.1016/j.jhazmat.2025.139875
Received 20 June 2025; Received in revised form 3 September 2025; Accepted 13 September 2025
Available online 14 September 2025

during the activated sludge process is driven by the formation of heteroagglomerates, with differential sedimentation being more important than fluid shear.

1. Introduction

Microplastic particles (MPs), defined as particulate plastic with dimensions between 1 μm and 1 mm [21], have been detected across many environmental compartments [23,29,34,37], essentially reflecting the high environmental persistence of conventional polymers. Microplastic particles discharged to wastewater are transported in sewer pipes to wastewater treatment plants (WWTPs). Representing the interface between the technical and the natural environment, WWTPs act as a critical barrier to remove MPs from the wastewater. Effective removal lowers the flux of MPs released with WWTP effluent to surface waters [4, 41,42]. However, given the accumulation of MPs in the sewage sludge combined with the environmental persistence of these MPs, the application of sludge to agricultural fields likely becomes an important pathway for MPs to the environment [27,33,43]. To estimate these fluxes, it is important to understand the fate of MPs in WWTPs.

The activated sludge process represents an integral part of contemporary wastewater treatment. Wastewater continuously enters aerated and stirred reactors containing suspended particulate biomass so-called flocs, which are typically in the size range of 100 to 200 μm [18]. In these aerated reactors, organic matter is degraded, ammonium is oxidized to nitrate (nitrification) and further converted to molecular nitrogen (denitrification), and organic and mineral particulate materials are enmeshed in sludge flocs (flocculation). After the aeration phase, the mixture of flocs and water referred to as sludge enters a sedimentation tank where the solids are separated from the water through sedimentation. The supernatant from the sedimentation tank (i.e., clarified water) typically containing ~5–10 mg L^{-1} of total suspended solids (TSS) is discharged into surface waters either directly or after a tertiary treatment such as sand filtration [18].

Previous studies mostly reported removals of at least 90 % of the total number of MPs from the wastewater stream during the wastewater treatment, indicating an effective transfer of the MPs to the sewage sludge [4,41,42]. Yet, the polymer types and size distribution of the MPs detected in the influent and the effluent water often differed [36,49]. These differences may reflect specific removal mechanisms that depend on the physicochemical properties of the MPs or may result from analytical shortcomings. The accurate quantification of MPs concentrations in WWTPs (i.e., sewage sludge, influent and effluent water) is challenging due to large uncertainties associated with representative sampling and lack of robust analytical methods. This resulted in reported MP concentrations spreading over several orders of magnitudes for WWTP effluents [28].

Based on experimental evidence obtained for the removal of engineered nanoparticles [25], microfibers [14], and nanoplastics [1,14] during the activated sludge process, we speculate that the formation of heteroagglomerates between sludge flocs and MPs plays a key role in transferring the MPs from the wastewater to the sludge. Several studies have also suggested that heteroagglomeration is important for the removal of MPs from wastewater [10,11,4,42], a hypothesis further supported by microscopic images showing MPs embedded in sludge flocs [10,11]. Yet, mechanistic understanding of the process remains limited. For example, the impact of different physicochemical properties including size, shape, polymer type and surface alterations resulting from UV-light irradiation on the behavior of MPs during the activated sludge treatment has received limited attention. Moreover, although heteroagglomeration of MPs with sludge flocs has been mentioned as key to the MP removal from wastewater, the relative importance of differential sedimentation and fluid shear to the formation of heteroagglomerates remained unexplored and the kinetics of this process poorly investigated.

The goals of this study were, therefore, (1) to assess the impact of MP size, polymer type, shape and UV-light irradiation on the MP removal in batch experiments simulating the activated sludge process, (2) to estimate the relative importance of differential sedimentation and fluid shear regarding the formation of heteroagglomerates, (3) to study the kinetics of heteroagglomeration of MPs during the activated sludge process, and, based on the experimental data, (4) to evaluate whether activated sludge serves as a non-specific accumulator for MPs entering the activated sludge process. As our experiments were designed to assess the impacts of varying properties of the MPs on their behavior during the activated sludge process, we systematically varied the properties (size, polymer type, morphology, UV-light irradiation) of the MPs, but kept the properties of the sludge matrix (e.g, pH, ionic strength, content, and composition of extracellular polymer substances) unchanged.

2. Materials and methods

2.1. Chemical reagents, filter materials and microplastic particles

Hydrogen peroxide (H_2O_2 35 %, Roth, order number: 9683.5), iron sulfate ($FeSO_4 \cdot 7\ H_2O$, Roth, Pro analysis, 2619776) and protocatechuic acid (Sigma, 37580–25g-F) were used to isolate the MPs after the experiments. Rinsing of all reaction vessels and sampling tools (e.g., steel mesh) before and after the analysis was performed with ethanol (70 %, Reuss Chemie, RC-FSP-018) and deionized (DI) water (Arium Pro, Sartorius). Stainless steel meshes (pore size 25 μm and 47 mm diameter, Haver & Boecker OHG, Germany) and aluminum oxide filters (Anodisc, pore size 0.2 μm and 47 mm diameter, Whatman plc, UK) were used to separate the MPs from the liquid matrices.

Colored or fluorescent MPs of different polymer types (i.e., polyethylene (PE), polyvinyl chloride (PVC), and polystyrene (PS)), shapes (fragments versus spheres), and sizes ranging from 6 to 580 μm, were used (details in Table S1). These MPs are referred to as probe MPs, as they were used to quantify the heteroagglomeration of MPs with sludge flocs. In addition, MPs of different colors or fluorescence than the probe MPs were used as surrogate standards to evaluate MPs losses during sample handling and processing for subsequent analysis. The use of differently colored or fluorescent MPs enabled their unambiguous identification and quantification by automated optical microscopy. The MPs are displayed in Figure S1, S2, and S3 and their provider, use, and properties are summarized in Table S1.

2.2. UV-light irradiation and characterization of probe microplastic particles

A selected number of red PE (60 μm), blue PVC (40 μm), and violet PS (100 μm) (Table S1) probe MPs were UV-light irradiated (300 – 800 nm) to simulate the photochemical oxidation of the polymer surfaces during environmental weathering. An irradiation of 350 kWh m^{-2} was applied and considered sufficient to cover the UV-light irradiation of plastic items that are discarded in the environment by littering and reach the sewer system through rain events. The details of the UV-light irradiation procedure are described in the SI (Section 2). After UV-light irradiation, the probe MPs were characterized using Attenuated Total Reflection – Fourier Transform Infrared Spectroscopy (ATR-FTIR) analysis and the carbonyl index (CI), which was used as a proxy for the probe MP surface oxidation, was calculated [39]. Further details are given in the SI (Section 2).

2.3. Heteroagglomeration experiments

Two types of experiments were performed to investigate the fate of MPs during the activated sludge process. The first set of experiments, referred to as removal experiments, aimed to assess the impact of polymer type (PE, PVC, PS), shape (fragment, sphere), size and UV-light irradiation on the transfer of MPs from wastewater to the sludge during the activated sludge process. The second set of experiments, referred to as kinetic experiments, aimed to investigate the kinetics of MP-sludge floc heteroagglomeration and to estimate the relative importance of differential sedimentation induced and fluid shear induced heteroagglomeration. Activated sludge was collected from a pilot WWTP operated at Eawag (described in [26]) on the day of the experiments. The pH of the collected activated sludge fluctuated between pH 7.8 and 8.1. A run table of all experiments including additional information about the probe MPs and the surrogate standards used in the individual experiments is provided in Table 1.

2.3.1. Experiments addressing the transfer of microplastic particles from wastewater into sludge during the activated sludge process (removal experiments)

Between 4'000 and 6'000 pristine or UV-light irradiated probe MPs (PE (60 μm), PS (100 μm), PVC (40 μm)) of unique colours were spiked into either activated sludge or into DI water. The experiments conducted in DI water served as control. Each polymer type was spiked individually for each experiment. A schematic of the experiments is given in Fig. 1A.

For each experiment, the number of added MPs was determined as follows: A small amount of probe MPs was deposited on a glass slide using a steel needle. The number of MPs deposited on the glass slides were determined by automated optical microscopy (VHX-7000, Keyence, Japan). The glass slide was then rinsed with 5 mL DI water to transfer the probe MPs into a 250 mL Schott bottle. Following this rinsing, each glass slide was imaged again under the optical microscope to check for remaining MPs and the total amount of MPs added to the Schott bottle was corrected accordingly. After adding the probe MPs to the Schott bottles, 200 mL of activated sludge or of DI water was transferred into the Schott bottles. Each bottle was then continuously mixed using a magnetic stirrer and aerated through glass Pasteur pipettes, which were inserted into the sludge and connected to the pressurized air outlet of the laboratory. Oxygen (O) concentration was kept above 5 mg O_2 L^{-1} at all times. The velocity gradient $\overline{G}$ due to stirring was estimated at 82 s^{-1}. The estimation does only include the power input due to stirring and thus reflects a minimum value (SI, Section 4). After an aeration and mixing period of 120 min, the content of the bottles was transferred into a 500 mL glass separation funnel for 30 min of sedimentation. The sludge remaining in the bottles was also rinsed with 10 mL of DI water into the separation funnel. Mixing and settling times were similar to those of full-scale activated sludge systems [44]. After sedimentation, the sedimented sludge was collected in a 600 mL glass beaker from the bottom of the funnel through the funnel outlet and the supernatant was subsequently drained through the same outlet into a separate 600 mL glass beaker. The emptied separation funnel was rinsed with 10 mL DI water and the wash water was added to the beaker containing the supernatant. In control experiments conducted with DI water, separation funnels were emptied and two volumes each of ~110 mL were collected corresponding to those of supernatant and sedimented sludge in experiments conducted with activated sludge. All experiments were conducted in triplicate. A run table of all removal experiments including the amounts of spiked and recovered probe MPs is provided in the SI (Table S2).

Table 1
Summary of all experiments conducted, providing an overview of the matrix, the probe microplastic particles (MPs), and the surrogate standards used. Experiments conducted in deionized (DI) water served as controls. The removal experiments (addressing the transfer of MPs from wastewater into the sludge during the activated sludge process) and the kinetic experiments (addressing the kinetics of the heteroagglomeration process) are described in Sections 2.3.1 and 2.3.2, respectively. In the kinetic experiments, either two or three different types of probe MPs were added as mixtures to the activated sludge samples to reduce the total number of reactors that had to be operated in parallel. PE: polyethylene, PVC: polyvinyl chloride, PS: polystyrene.

Type of experiment	Matrix	Probe MPs	Surrogate standards
Removal	DI water	Red PE (60 μm)	Blue PE (60 μm)
Removal	DI water	Blue PVC (40 μm)	Red PE (60 μm)
Removal	DI water	Violet PS (100 μm)	Red PE (60 μm)
Removal	Sludge	Red PE (60 μm)	Blue PE (60 μm)
Removal	Sludge	Blue PVC (40 μm)	Red PE (60 μm)
Removal	Sludge	Violet PS (100 μm)	Red PE (60 μm)
Removal	Sludge	UV-irradiated red PE (60 μm)	Blue PE (60 μm)
Removal	Sludge	UV-irradiated blue PVC (40 μm)	Red PE (60 μm)
Removal	Sludge	UV-irradiated violet PS (100 μm)	Red PE (60 μm)
Kinetic	Sludge	Red PE (60 μm), Blue PVC (40 μm), Violet PS (100 μm)	Green PE (60 μm)
Kinetic	Sludge	UV-irradiated red PE (60 μm), UV-irradiated blue PVC (40 μm), UV-irradiated violet PS (100 μm)	Green PE (60 μm)
Kinetic	Sludge	Fluorescent yellow PS (6 μm) Blue PE (24 μm)	Fluorescent Nile Red PS (11 μm)
Kinetic	Sludge	Blue PE (580 μm) Red PS (460 μm)	Pink PE (540 μm)

2.3.2. Experiments to evaluate the kinetics of heteroagglomeration (kinetic experiments)

Experiments to study the kinetics of the formation of heteroagglomerates between MPs and sludge flocs during the activated sludge process were conducted in a similar manner as the experiments described in Section 2.3.1 (removal experiments). However, in these (kinetic) experiments, the aeration and mixing times were 0, 1, 5, 15, 30, 60 and 120 min, whereas the sedimentation time of 30 min was kept constant for all experiments. A schematic of the kinetic experiments is given in Fig. 1B. In addition to using the same set of probe MPs as for the removal experiments, the size range of the MPs used for the kinetic experiments was expanded from 40 – 100 μm to 6 – 580 μm to assess the potential size dependence of the heteroagglomeration process in more detail (Table 1). Because of the numerous mixing and aeration times tested, the probe MPs were added as a mixture of either two or three different MPs types (Table 1) to the Schott bottles to ensure that the total number of reactors ran in parallel remained feasible. The concomitant addition of different types of probe MPs unlikely affected the heteroagglomeration rates between probe MPs and sludge flocs (e.g., through the formation of MP-MPs agglomerates), because the number of sludge flocs in the system was much higher than the number of probe MPs added.

The number of spiked probe MPs > 20 μm was determined as described above for the colored probe MPs and ranged from ~250 to ~1'000. For the smaller MPs (6 μm probe MPs and 11 μm surrogate standards), the number of spiked MPs was derived from dilutions made from certified stock suspension. The experimental details are described in the SI (Section 5). Approximately 40'000 and 10'000 of the 6 and 11 μm probe MPs, respectively, were added.

All experiments were conducted in triplicates. In the kinetic experiments, only the supernatant was collected and investigated for the presence of probe MPs. This approach was chosen to reduce the number

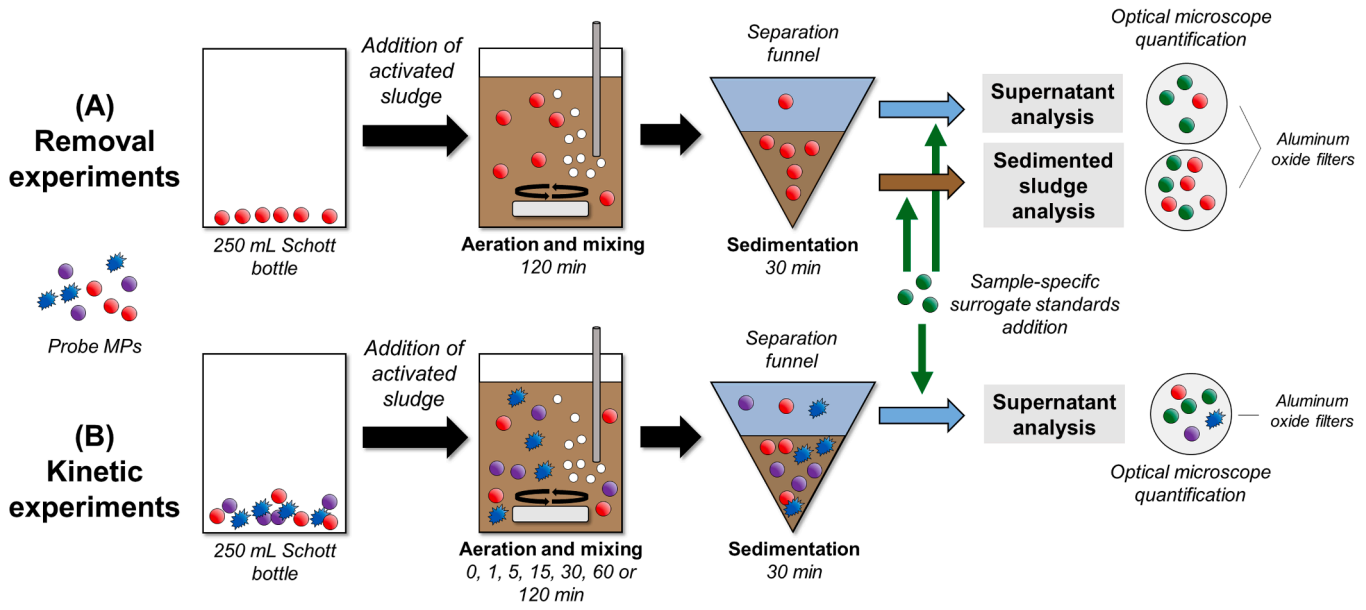

Fig. 1. Schematic of (A) the experiments addressing the removal of microplastic particles (MPs) during the activated sludge process (removal experiments) and (B) the experiments to evaluate the kinetics of the formation of heteroagglomerates between MPs and sludge flocs and to estimate the relative importance of differential sedimentation and fluid shear regarding the formation of heteroagglomerates (kinetic experiments). Control experiments were conducted in DI water (not shown).

of samples to analyze, as results from the removal experiments showed that supernatant analysis provided complementary information to sedimented sludge analysis. The relevant data of these experiments are listed in respective run tables in the SI (Table S3, S4, S5, and S6).

2.4. Sample processing and quantification of the microplastic particles

The processing steps for supernatants and sedimented sludge samples are summarized schematically in Fig. 2 and described in more detail in the following sections.

2.4.1. Supernatants

The supernatants collected in 600 mL glass beakers were sonicated for 30 s in an ultrasonic bath (Biolock 88155 Ultrasonic Cleaner, 35 kHz) to facilitate their subsequent filtration through a 47 mm diameter steel mesh with a nominal 25 µm pore size cutoff. The solids

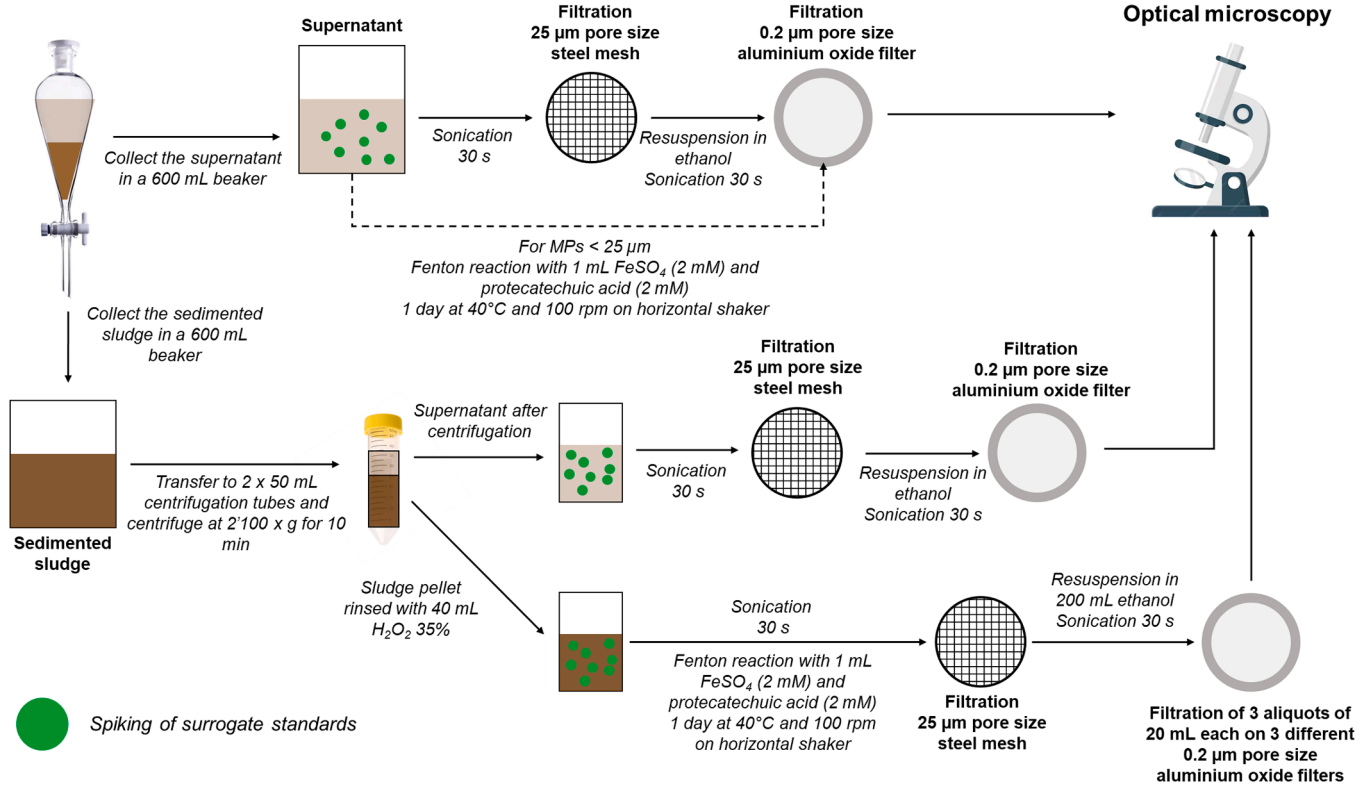

Fig. 2. Schematic of the processing steps to extract the probe microplastic particles (MPs) from the experimental samples. Additions of surrogate standards are indicated by the green dots.

and MPs retained on the mesh were resuspended by immersing the steel mesh in ethanol in a glass beaker while sonicating for 30 s in an ultrasound bath. The suspension was then filtered on a 47 mm Anodisc filter.

In the experiments using MPs smaller than 25 μm, stainless steel sieves deemed impractical to isolate the MPs from the supernatants. Therefore, the supernatants were incubated with H_2O_2 to digest remains of organic material / flocs from the activated sludge, instead of filtering the samples on a stainless steel mesh. For the digestion, 40 mL of H_2O_2 were added to the glass beakers containing the supernatants. One mL of $FeSO_4$ (2 mM) was added to catalyze a Fenton reaction and 1 mL of protecatechuic acid (2 mM) to prevent the precipitation of iron colloids. The reaction was conducted in an incubator-horizontal shaker (Heidolph, Unimax 1010) at 40°C and 100 rpm for 24 h. The digested samples were sonicated for 30 s and afterwards filtered on 47 mm Anodisc filters.

For the quantification of the probe MPs as well as the surrogate standards $>$ 20 μm on Anodisc filters, the entire surface area of the Anodisc filters was imaged with an automated optical microscope (VHX-7000, Keyence, Japan) and both probe MPs and surrogate standards were identified based on their unique colors and shapes. For the fluorescent probe MPs and surrogate standards ($<$ 20 μm), a fluorescence adapter was mounted on the optical microscope and an area covering 27–48 % of the total filter surface was imaged (Table S5). The number of fluorescent probe MPs and surrogate standards quantified on the analyzed filter area was then scaled to the total filter area. Examples of Anodisc filters following filtration of supernatants are provided in Figures S5, S7, and S8.

2.4.2. Sedimented sludge

Sedimented sludge, referring to the sludge that accumulated at the bottom of the separation funnel after 30 min of sedimentation, was collected in a 600 mL glass beaker. The sedimented sludge was then transferred into two 50 mL centrifugation tubes and centrifuged at 2'100 x g for 10 min to dewater it. The volume of sedimented sludge sometimes exceeded the volumes of the centrifugation tubes by 5 to 10 mL. In this case the 'excess' volume of sedimented sludge was kept in the glass beaker. The supernatant resulting from the centrifugation, referred to as centrifuged supernatant, was transferred into another 600 mL glass beaker and processed as described above (Section 2.4.1).

The sludge pellets formed after centrifugation in the two centrifugation tubes were combined by rinsing them with a total of 40 mL of H_2O_2 into the glass beaker where the sedimented sludge was collected. One mL of $FeSO_4$ (2 mM), and 1 mL of protecatechuic acid (2 mM) were added to the beaker to catalyze a Fenton reaction as described in section 2.5.1 and Fig. 2. Following a reaction time of 24 h at 40°C, the suspensions were sonicated for 30 s and afterwards filtered through a 47 mm steel mesh (pore size 25 μm). The mesh was immersed in 200 mL of ethanol in a glass beaker and sonicated for 30 s to resuspend the solids and the MPs retained on the mesh. Three aliquots of each 20 mL (corresponding to 3 $\times$10 % = 30 % of the total volume of the suspension) were filtered on three separate Anodisc filters for automated MP detection using optical microscopy. The MPs were quantified as described in 2.4.1 and the total number of MPs in the sludge pellets were extrapolated from the total number of MPs detected on the three Anodisc filters which corresponded to 30 % of the sludge pellets.

The total number of probe MPs in the sedimented sludge corresponds to the sum of the probe MPs in the supernatant of the centrifuged sludge (centrifuged supernatant) and the probe MPs detected in the sludge pellets. An example of an Anodisc filter resulting from the sludge pellets is provided in Figure S6.

2.5. Surrogate standards for quality assurance and quality control (QA/QC) measures

After separating the supernatant, the centrifuged supernatant and the sludge pellets following the heteroagglomeration experiment, a known number of surrogate standards were added individually to these compartments (the same method as described in Section 2.4.1 was applied to quantify the amount of surrogate standards that was added). The purpose of this approach was to assess the potential losses of probe MPs during further sample processing (Fig. 1 and Fig. 2), as described in [35]. The surrogate standards were unambiguously identified by their unique color or fluorescence which allowed their quantification in the different compartments (supernatant, sludge pellet, and centrifuged supernatant). For example, in experiments using red PE spheres as probe MPs, blue PE spheres were used as surrogate standards (Table 1). Surrogate standards recoveries are reported but were not used to correct the recoveries of the probe MPs.

The number of spiked and recovered surrogate standards is provided in Table S2, S3, S4, S5, and S6. In control experiments where neither probe MPs nor surrogate standards were spiked to the activated sludge (n = 3), neither probe MPs nor surrogate standards were identified, demonstrating that background MPs from the activated sludge did not result in false positives (SI, section 12).

2.6. Experiments to determine the total suspended solids (TSS)

The TSS mass concentration of the activated sludge that was collected from the WWTP was determined on the day of the experiment according to the standard method [5]. The details are described in the SI (Section 11). This TSS concentration was corrected for the addition of DI water (5 mL for the removal experiments and 5 mL for each probe MP type in the kinetic experiments, summing up to either 10 or 15 mL, depending on the number of different probe MPs) that was added when spiking the MPs to the Schott bottles used for experiments with the activated sludge (Table S7). Additionally, analogous experiments were conducted (200 mL sludge, 120 min of aeration and mixing time, 30 min of sedimentation) using the same activated sludge as used for the removal experiments, but without spiking neither probe MPs nor surrogate standards. These experiments provided information about the TSS content of the supernatant and of the sedimented sludge.

3. Results and discussion

3.1. UV-light irradiation of microplastic particles

UV-light irradiation of the MPs over 500 h led to a variable bleaching of the purple PS probe MPs (100 μm), whereas the colors of the red PE (60 μm) and the blue of PVC (40 μm) remained unaffected (Figure S1). Scanning electron microscopy images of selected pristine and UV-light irradiated probe MPs showed that UV-light irradiation had little effect on particle surface morphology (Figure S1). The results of ATR-FTIR measurements (Figure S4) supported the findings from the microscopy analyses: the CI of PS significantly increased (Student's *t*-test, p-value = $3.4{\cdot}10^{-5}$) after UV-light irradiation whereas the latter had no effect on the CI of PE and PVC (p-values $>$ 0.2, Fig. 3).The CI increase for probe PS 100 μm MPs suggests the formation of carbonyl groups, reflecting oxidation reactions on the PS surface. Several studies have reported that an increase in CI is correlated with a decrease in water contact angle, suggesting that the particle surface became increasingly hydrophilic [15,3,40,9]. The ATR-FTIR measurements thus strongly suggest that UV-irradiation rendered PS more hydrophilic while PE and PVC most likely remained hydrophobic. The reason for the higher degree of weathering observed for PS compared to the other MP types is most likely the phenyl ring which efficiently absorbs UV and visible light. This leads to radicals formation and chain scissions accelerating the polymer degradation [16].

3.2. Removal experiments

These removal experiments (120 min aeration and mixing, followed by 30 min of sedimentation) aimed to mimic an activated sludge process

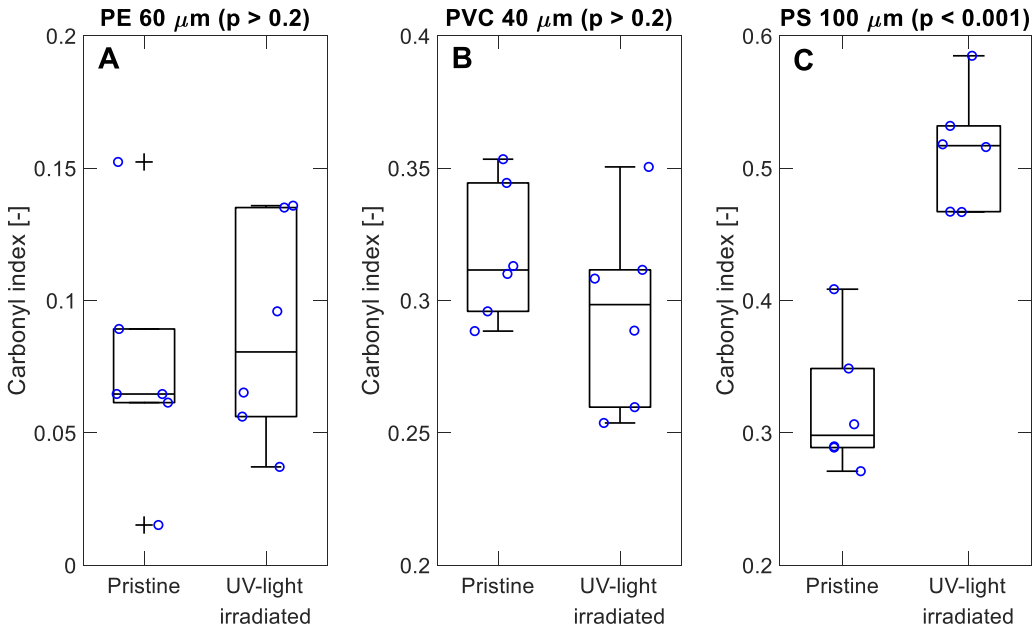

Fig. 3. Carbonyl Indices (CI) of pristine (n = 6) and UV-light irradiated (n = 6) (A) polyethylene (PE) 60 μm, (B) polyvinyl chloride (PVC) 40 μm, and (C) polystyrene (PS) 100 μm probe MPs. The horizontal line at the center of each box corresponds to the median value. The bottom and top of each box indicate the 25th and 75th percentiles. Outliers are indicated by a '+ ' if they are 1.5 times (75th – 25th percentiles) above the top or below the bottom of the boxes. The whiskers connect the box to the last non-outlier values. Individual measurements points are indicated with blue dots.

in full-scale WWTPs, with an aeration reactor followed by a secondary clarifier. In the following, we first present the data on the recoveries of the surrogate standards and then discuss the transfer of the different MP types from the wastewater to the sludge during the activated sludge process.

3.2.1. *Recoveries of surrogate standards*

The recoveries of surrogate standards were above 70 % (Fig. 4A-C), except for the bottom layer sample in the experiment with DI water and probe PE 60 μm MPs, in which only about 60 % of the added surrogate standards were recovered. However, the recoveries of 60 % of the surrogate standards do not substantially affect the overall number balance as only 2 % of the probe PE 60 μm MPs added in this experiment were found in the bottom layer (Fig. 4D). Although surrogate standards recoveries of 70 % may appear low, they align well with the few available data on recoveries reported previously [20,7]. Note that most MP studies still lack number-based MP recoveries.

3.2.2. *Removal of pristine probe microplastic particles (40 to 100 μm) in deionized water*

In the control experiments conducted in DI water to determine the distribution of probe MPs in the water column without activated sludge, half of the liquid volume (~110 mL) was withdrawn from the bottom of the separation funnel at the end of the experiments to constitute the bottom layer. This volume corresponds to the volume of sedimented sludge removed in experiments conducted with activated sludge (Fig. 4). The remaining water in the funnel (~110 mL) constituted the upper layer in Fig. 4. Experiments with DI water were only conducted with pristine probe MPs.

More than 80 % of the probe PE 60 μm MPs added floated to the upper layer (Fig. 4D), whereas less than 2 % were found in the bottom layer. This finding is consistent with PE being slightly positively buoyant and thus, the majority of the probe PE 60 μm MPs was expected in the upper layer. Considerably larger percentages of added probe PVC 40 μm and probe PS 100 μm MPs (i.e., 33 % and 45 % of the added probe MPs, respectively) were found in the bottom layer. The percentages of MPs detected in the bottom layer correspond to the fractions expected to settle gravitationally in the absence of heteroagglomeration with sludge flocs. Both PVC and PS have a higher density than water and following calculations using Stokes' law (Figure S13), should have sedimented to the bottom layer of the funnel (distance to reach the bottom layer: 15 cm) within the settling time of 30 min. However, the high interfacial binding energy of hydrophobic probe MPs such as PS and PVC, to the air-water interface may explain their presence in the upper volume [2]. Pristine PVC fragments had a rough surface morphology (Figure S1) which may contain tiny gas bubbles [13]. Gas bubbles would also have lowered the effective density of the PVC fragments and may thus explain the presence of probe PVC 40 μm MPs in the upper part of the funnel.

3.2.3. *Removal of pristine probe microplastic particles (40 to 100 μm) in activated sludge*

In experiments conducted with activated sludge, more than 80 % of the spiked probe PE, PVC, and PS MPs were recovered (Fig. 4E). At least 90 % of the probe MPs recovered were associated with the sedimented sludge (centrifuged supernatant and sludge pellet combined, Fig. 4H) demonstrating the efficient transfer of the probe MPs into the sludge matrix. These MPs have sedimented along with the sludge flocs likely through the formation of heteroagglomerates, suggesting that heteroagglomeration plays a key role in the transfer of MPs from wastewater to sludge.

The impact of the heteroagglomeration is most obvious for the probe PE 60 μm MPs. This is related to the density of the probe PE 60 μm MPs, which is lower than the density of water. Thus, in the absence of water, only a negligible amount of probe PE 60 μm MPs were found in the bottom layer (in experiments conducted with DI water), and the formation of heteroagglomerates resulted in an efficient accumulation of the PE MPs in the sewage sludge. This topic is discussed in more detail in Section 3.3.6 (Mechanisms of heteroagglomeration in activated sludge).

The sludge centrifugation resulted in a release of about 10 % of the probe PE 60 μm MPs from the sludge flocs and the majority of the probe MPs remained attached to the sludge flocs. The released probe PE 60 μm MPs buoyantly rose to the water surface and were, thus, detected in the centrifuged supernatant (Fig. 4E). The dominant fraction of MPs remained attached to the sludge flocs further supporting the hypothesis that MP – flocs heteroagglomerates were formed during the simulated activated sludge treatment. Given that the densities of PS and PVC

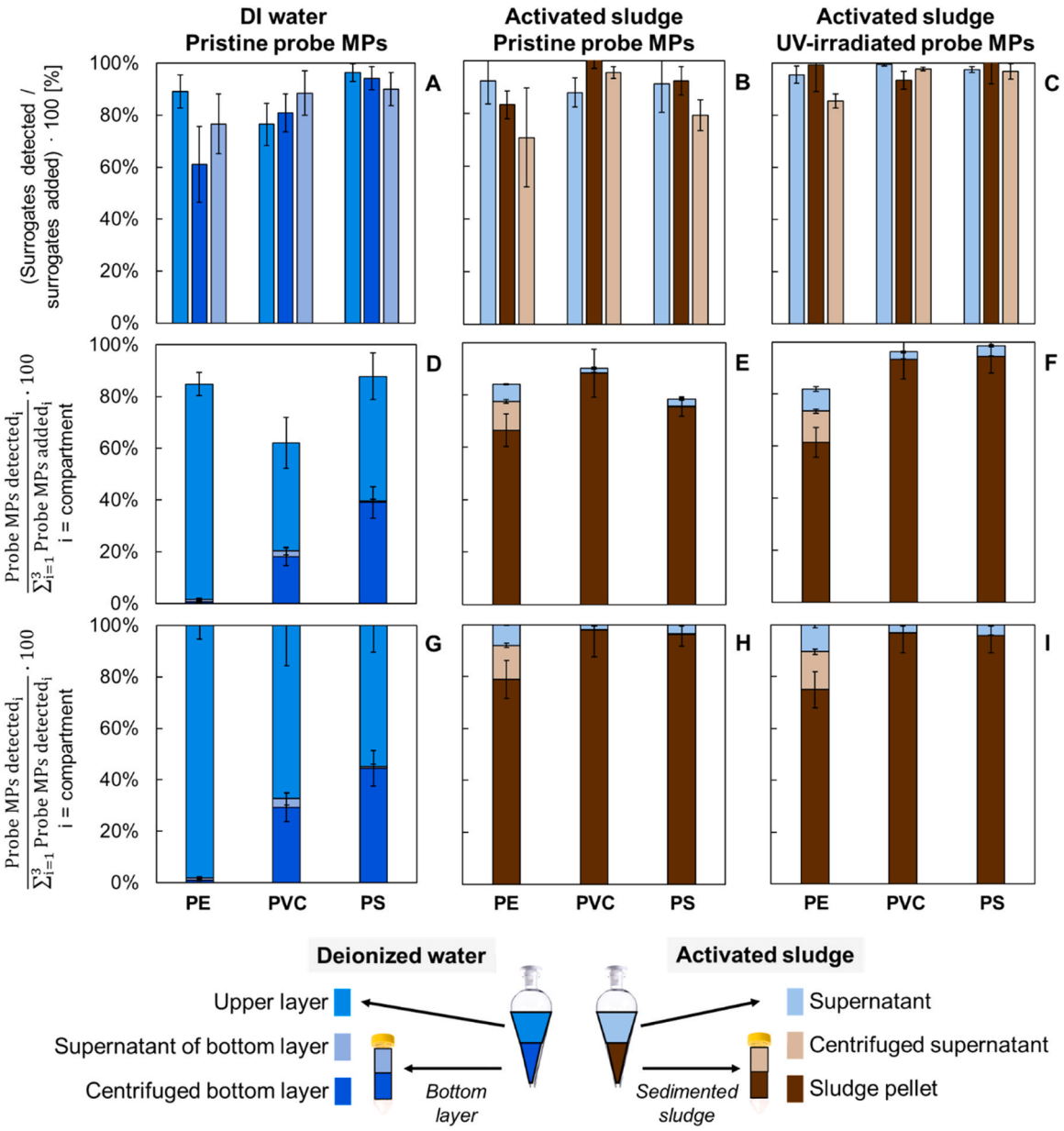

Fig. 4. Recoveries of surrogate standards spiked individually to the supernatant, the centrifuged supernatant, and the sludge pellets before further processing of the samples (A-C). Fractions of the probe MPs (polyvinyl chloride (PVC, 40 μm), polystyrene (PS, 100 μm) and polyethylene (PE, 60 μm)) summed over the three compartments (supernatant, centrifuged supernatant, and sludge pellet), relative to the total amount of probe MPs spiked (D-F). Fractions of the probe MPs (PVC (40 μm), PS (100 μm) and PE (60 μm)) summed over the three compartments (supernatant, centrifuged supernatant, and sludge pellet), relative to the total amount of probe MPs detected (G-I) Note that surrogate standard recoveries represent quality control / quality assurance measures and address the sample losses related to processing of different matrices. The cumulative recoveries of the probe MPs represent the overall recoveries of spiked probe MPs. Individual panels refer to experiments with pristine probe MPs in deionized (DI) water (A, D, G), pristine probe MPs in activated sludge (B, E, H), and UV-light irradiated probe MPs in activated sludge (C, F, I). The total number of probe MPs that sedimented in the funnel corresponds to the sum of the probe MPs quantified in the supernatant of the centrifuged sludge (centrifuged supernatant) and in the sludge pellets. In the experiments with DI water, the upper layer corresponds to the supernatant and the bottom layer corresponds to the sedimented sludge, whereas the volumes of the upper and the bottom layers are ~110 mL each. Error bars represent the standard deviations (1 x σ, n = 3).

exceed that of water, the respective MPs were only found in the sludge pellet and were absent in the centrifuged supernatants (Fig. 4E).

3.2.4. *Removal of UV-light irradiated probe microplastic particles (40 to 100 μm) in activated sludge*

Similar trends as observed for the experiments with pristine probe MPs were observed in the experiments with UV-light irradiated probe MPs in activated sludge: More than 80 % of the added probe MPs were recovered (Fig. 4F), of which most (> 90 %) were associated with sedimented sludge (Fig. 4I). The number of UV-light irradiated probe PS 100 μm MPs recovered in the sedimented sludge (> 90 %) was higher than that of pristine probe PS 100 μm MPs recovered (80 %, Fig. 4E/F). This can be explained by the higher surrogate standards recoveries obtained for the experiments conducted with the UV-light irradiated probe PS 100 μm MPs compared to the experiments conducted with pristine probe PS 100 μm MPs (Fig. 4 B/C). The observed differences in probe PS 100 μm MPs recoveries, thus, rather reflect different losses of probe PS 100 μm MPs during sample processing than chemical changes induced by UV-light irradiation. The relative fraction of added probe MPs recovered in the supernatant was highest for PE (10 %), followed by PS

(4 %) and PVC (3 %) (Fig. 4I). Similar results were also obtained from the experiments conducted with the pristine probe MPs (Fig. 4H), suggesting that UV-light irradiation did not affect the transfer of the MPs to the sludge matrix during the activated sludge process.

3.2.5. *Microplastic particle recovery versus total suspended solids*

The fractions of pristine and UV-irradiated probe MPs recovered from the supernatant relative to the total number of probe MPs recovered (from Fig. 4H-I) were plotted against the mass of TSS in the supernatant relative to the total mass of TSS in the activated sludge (Fig. 5). The data points for PS and PVC project close to the 1:1 line (Fig. 5), indicating that the probe MPs found in the supernatant were associated with the (residual) suspended flocs (i.e. the TSS in the supernatant). Furthermore, the probe PS 100 μm or PVC 40 μm MPs concentration ($\#_{\text{probe MPs}}\ g_{\text{TSS}}^{-1}$) in the supernatant was similar to the probe MPs concentration in the sedimented sludge (Table S7). This finding indicates an even loading of the TSS with MPs, further supporting the hypothesis that MPs undergo efficient heteroagglomeration. However, the data points for PE project above the 1:1 line in Fig. 5 (inset), suggesting that some probe PE 60 μm MPs remained freely dispersed in the supernatant.

The experiments were conducted at different activated sludge concentrations ranging between 1.8 and 4.1 gTSS L^{-1}. Yet, the probe MPs (being pristine or UV-light irradiated) efficiently heteroagglomerated with the sludge flocs and accumulated in the sedimented sludge to a similar extent (Table S7). Given that the concentrations of TSS in full-scale activated sludge systems usually range between 2 and 4 gTSS L^{-1} [44], the activated sludge process is expected to efficiently transfer the MPs from the wastewater to the sludge at all conditions.

This set of (removal) experiments demonstrated that after 120 min of mixing and aeration and followed by 30 min of sedimentation, > 90 % of the probe MPs recovered were found in the sedimented sludge, independent of polymer type (PS, PE, PVC), shape (sphere or fragments) or whether the probe MPs were pristine or UV-light irradiated. However, with 8–10 % of the probe PE 60 μm MPs remaining in the supernatant, the PE fraction in the supernatant was higher compared to respective fraction of TSS remining in the supernatant (2–4 %).

Since only one aeration and mixing time point was tested, the kinetics of the formation of heteroagglomerates between probe MPs and sludge flocs and the minimum aeration and mixing time required to reach a steady-state (i.e. constant concentrations of MPs in the supernatant) were not accessible. Therefore, we conducted additional experiments with varying aeration and mixing times but maintaining the sedimentation time constant (30 min).

3.3. *Kinetic experiments*

Kinetic experiments with aeration and mixing times ranging from 0 min to 120 min followed by a constant sedimentation step of 30 min were conducted. The probe MPs were quantified in the resulting supernatants (Fig. 1 and Fig. 2). In addition to the set of probe MPs used in the previous experiments, the size range of the probe PE and PS MPs was expanded to 6 – 580 μm, allowing a more detailed assessment of the impact of the MP size on the heteroagglomeration kinetics. Optical images of the probe MP-sludge flocs heteroagglomerates are provided in the SI (Section 9, Figures S9-S12).

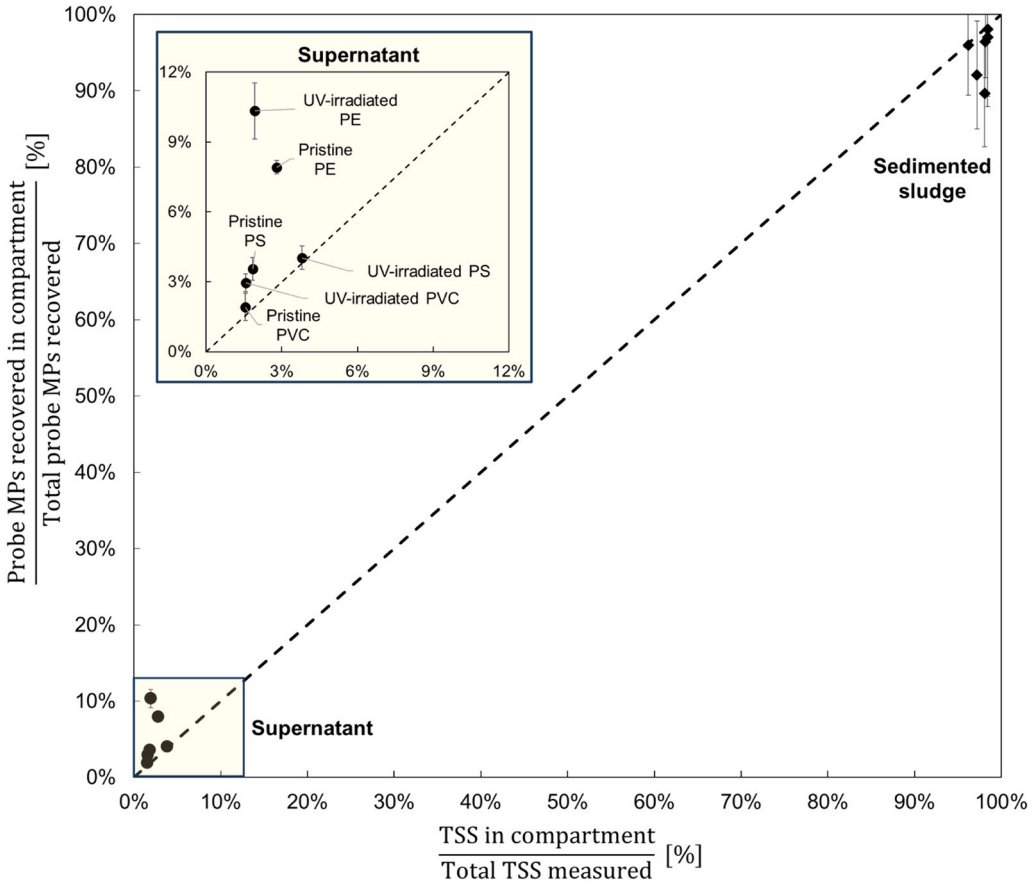

Fig. 5. Pristine and UV-light irradiated probe microplastic particles (MPs; polyethylene (PE), polyvinyl chloride (PVC) and polystyrene (PS)) quantified in the supernatant (filled circles) or sedimented sludge (filled diamonds) relative to the total number of probe MPs recovered in the experiments against the mass of total suspended solids (TSS) measured in the supernatant or in the sedimented sludge relative to the total mass of TSS in the activated sludge. The inset (yellow square) shows the polymer specific data for the supernatants. The error bars refer to the standard deviations (1 x σ, n = 3). The dashed line corresponds to a 1:1 ratio.

3.3.1. Recoveries of surrogate standards

The recoveries of the surrogate standards from all kinetic experiments were mostly above 80 % (Fig. 6E-H). The more pronounced variations in recoveries ranging from 70 to 130 % from the smallest surrogate standards (Fig. 6G) reflect the uncertainties in the analysis of recovered MPs < 20 µm (e.g., the number of particles spiked was estimated based on the pipetted volume of the stock suspension, see section 2.6.2, and the number of particles recovered was extrapolated based on

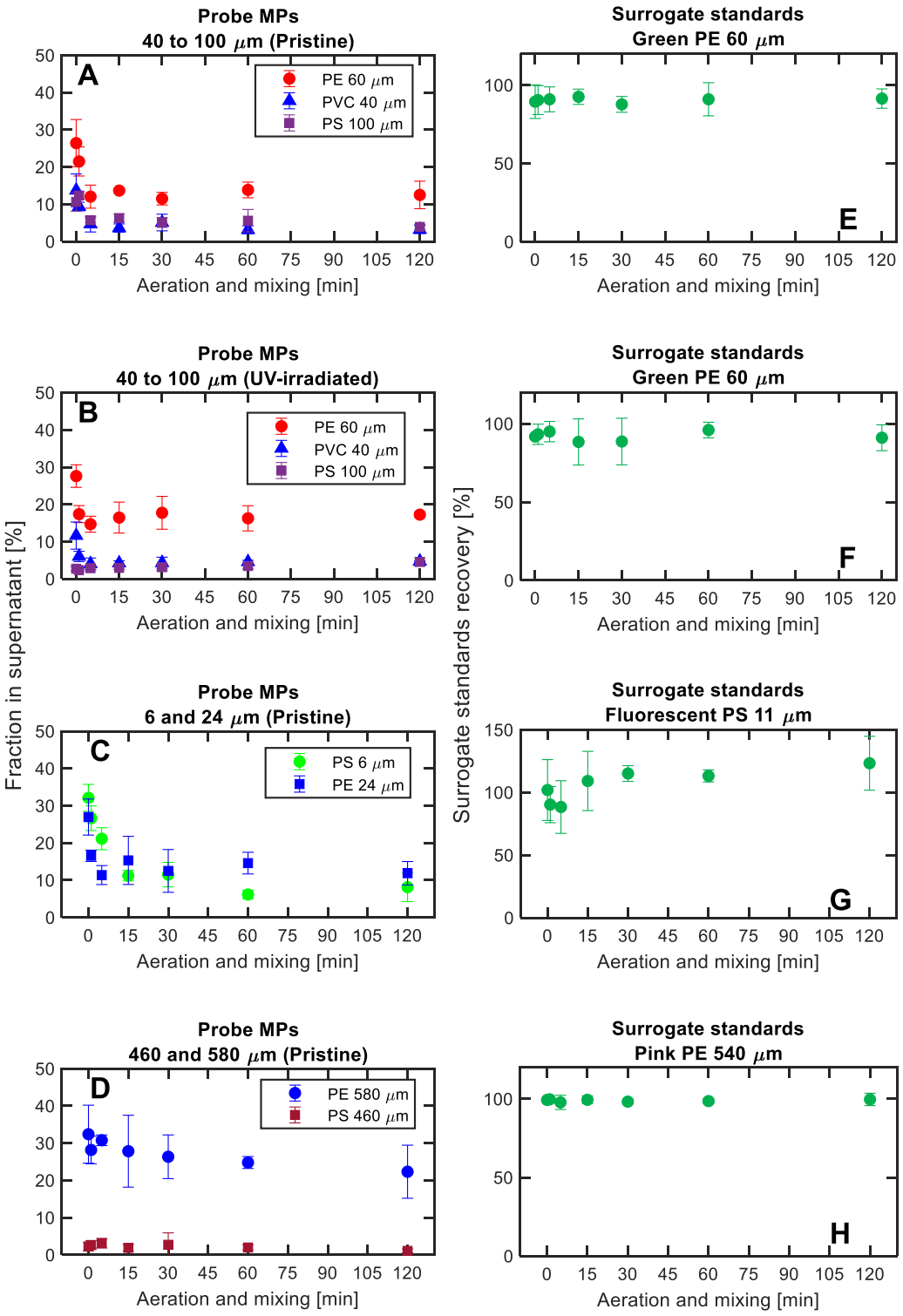

Fig. 6. Number of probe microplastic particles (MPs) quantified in the supernatant relative to the number of probe MPs added in experiments conducted with (A) pristine probe MPs (40 to 100 µm), (B) UV-light irradiated probe MPs (40 to 100 µm), (C) pristine probe MPs (6 and 24 µm), and (D) pristine probe MPs(460 and 580 µm) plotted against the aeration and mixing time. Note that all experiments included a 30 min sedimentation step that followed the indicated aeration and mixing times. Panels A and B address the impact of MP type, morphology and extent of UV-light irradiation, and panels C and D address the impact of MP size on the removal efficiencies. Corresponding recoveries of surrogate standards spiked to the supernatants are given to the right. The following surrogate standards were used: (E) and (F): green PE (60 µm), (G): fluorescent PS (11 µm), and (H): pink PE (540 µm). The error bars correspond to one standard deviation (n = 3).

a subsampled area of the filter, see Section 2.4). Conversely, the recoveries of the largest surrogate standards (540 μm) were between 95 and 100 % (Fig. 5H).

3.3.2. Kinetics of heteroagglomeration of pristine probe MPs (40 to 100 μm)

Already after the shortest mixing and aeration time, denoted as 0 min (which however included a 30 min sedimentation time), only a small fraction of the probe MPs added (i.e., 26 % of PE, 11 % of PS, and 14 % of PVC) was recovered from the supernatant (Fig. 6A). Extensive removal resulted from both the sedimentation of the probe PS 100 μm and PVC 40 μm MPs themselves (densities > 1 g cm^{-3}), and the differential settling of probe MPs and sludge flocs, which likely led to the formation of heteroagglomerates. Limited mixing occurred during sample manipulation, which may also have resulted in the formation of heteroagglomerates. However, sample handling and the settling time of 30 min were identical for all experiments and, thus, had the same contribution to the observed removal kinetics. Within the first 5 min of aeration and mixing, the fraction of probe MPs in the supernatant decreased monotonously (Fig. 6A) indicating their increasing removal by heteroagglomeration with the sludge flocs, facilitated by mixing-induced fluid shear.

After ~5 min of aeration and mixing, the fraction of the added probe MPs that remained in the supernatant leveled off at values ~5 % for PS and PVC, and ~13 % for PE and further increase in mixing times did not result in additional removal of the spiked probe MPs from the supernatant (Fig. 6A). We ascribe this leveling off at non-zero values to heteroagglomeration being a reversible process. The steady state corresponds to the dynamic equilibrium between the formation and breakup of the heteroagglomerates [6] and to the amount of flocs-MPs heteroagglomerates that remain in the supernatant after 30 min of sedimentation. The fraction of total probe MPs added remaining in the supernatant was as follows: PE $>$ PS $\approx$ PVC, which is consistent with what was observed in the experiments with 120 min of mixing and 30 min of sedimentation time (Fig. 4).

3.3.3. Kinetics of heteroagglomeration of UV light irradiated probe MPs (40 to 100 μm)

The results of the kinetic experiments conducted with UV-irradiated probe MPs (40 to 100 μm) followed similar trends as observed for the pristine MPs (40 to 100 μm) (Fig. 6B). At the shortest aeration and mixing time evaluated, around 30 % of the spiked PE and 10 % of the spiked PVC were found in the supernatant. The fraction of PS, however, was already close to 5 % at this first time point, suggesting an almost instantaneous and complete formation of heteroagglomerates followed by their removal through sedimentation. During the first ~5 min of aeration and mixing followed by the 30 min sedimentation step, the fraction of probe PE 60 μm and PVC 40 μm MPs in the supernatant sharply decreased to values around 15 % and 5 %, respectively, similarly as observed for the experiments conducted with the pristine probe MPs. After this initial decrease, the fraction of UV-light irradiated probe MPs quantified in the supernatant remained constant (Student's test, $p > 0.05$).

The removal kinetics during the first 5 min were, thus, similar for UV-light irradiated and pristine probe PE and PVC MPs but differed for the UV-light irradiated probe PS 100 μm MPs compared to their pristine analogues. This is consistent with the fact that only probe PS 100 μm MPs displayed changes in properties after UV- light irradiation. To help rationalize the differences in heteroagglomeration for the probe PS 100 μm MPs, the zeta-potential of pristine (-3.8 $\pm$ 1.6 mV, $n = 6$) and UV-light irradiated PS (-4.9 $\pm$ 0.6 mV, $n = 6$) were determined in treated wastewater as surrogate for the water matrix used in these experiments (SI, section 13). The similarity of these values (Student's *t*-test, p-value = 0.14) indicates that the difference in negative charge is so small that it unlikely explains the different kinetic behavior between pristine and UV-light irradiated probe PS MPs.

Based on the increased CI of the UV-light irradiated probe PS 100 μm MPs, the PS became more hydrophilic than their pristine analogues. A fraction of the pristine, and, thus, hydrophobic probe MPs may have remained at the water-air interface and, therefore, only have had limited contact with the sludge flocs during the initial stage of mixing. By comparison, the UV-irradiated and, thus, more hydrophilic probe PS 100 μm MPs were probably evenly dispersed in the activated sludge. This would result in more frequent contacts and faster formation of heteroagglomerates with the sludge flocs from the onset of the experiment, which may explain the more rapid removal of the UV-light irradiated compared to the pristine probe PS 100 μm MPs.

3.3.4. Kinetics of heteroagglomeration of small pristine probe microplastic particles (6 to 24 μm)

The smaller pristine probe MPs (6 to 24 μm) exhibited a pattern similar to those of the pristine and UV-light irradiated probe MPs (40 to 100 μm) (Fig. 6C). With minimal mixing ($t = 0$ min), 32 % of the probe PS 6 μm MPs and 27 % of the probe PE 24 μm MPs added were recovered from the supernatant. These fractions decreased rapidly and stabilized at a plateau of ~13 % after 5 min of aeration and mixing for the probe PE 24 μm MPs and at ~10 % after 15 min for the probe PS 6 μm MPs. The longer times for the smallest probe MPs needed to attain steady state conditions likely results from the smaller sizes of the probe PS 6 μm MPs, lowering the collision probability and thus, collision frequency with the sludge flocs and therefore slowing down the heteroagglomeration process [17]. The residual amounts of PE and PS in the supernatant after 120 min were similar to those observed for the larger MPs (40 to 100 μm) discussed above, indicating that small MPs (6 μm in our study) and larger MPs (40 and 100 μm) are equally well transferred from the wastewater to the sludge during the activated sludge process.

3.3.5. Kinetics of heteroagglomeration of large pristine probe MPs (460 and 580 μm)

The heteroagglomeration pattern of the large, pristine MPs (460 and 580 μm) was different from that observed for smaller MPs. At $t = 0$ min, the fraction of total probe MPs added in the supernatant was ~3 % and 33 % for probe PS 460 μm and PE 580 μm MPs, respectively (Fig. 6D). This fraction remained constant for the probe PS 460 μm MPs over all experimental mixing and aeration times (Student's *t*-test, $p > 0.05$). The very efficient removal of PS can be attributed to their large size and negative buoyancy that resulted in their rapid sedimentation during the settling phase. On the other hand, the fraction of probe PE 580 μm MPs remaining in the supernatant reached ~23 % after 120 min of mixing and aeration, although the difference with $t = 0$ min was not significant (Student's *t*-test, $p > 0.05$). Even assuming an efficient heteroagglomeration between probe PE 580 μm MPs and sludge flocs, it is possible that some of the resulting heteroagglomerates were positively buoyant and, thus, remained in the supernatant during the settling phase.

3.3.6. Mechanisms of heteroagglomeration in activated sludge

To further explore the mechanisms that led to the accumulation of probe MPs in the sedimented sludge, data from the following experiments were considered: i) blank experiments conducted in DI water, ii) kinetic removal experiments at timepoint t_0, and iii) kinetic removal experiments once steady states conditions were reached. We have summarized the relevant data in Table S8.

Due to the density of probe PE 60 μm MPs, which is lower than the density of water, all of them were found in the upper layer in the blank experiments conducted in DI water. In the presence of sludge flocs (timepoint t_0 in kinetic removal experiments), only 25 % of the probe PE 60 μm MPs were found in the supernatant. The presence of the sludge flocs, thus, resulted in the removal of 75 % of the probe PE 60 μm MPs, most likely through the formation of heteroagglomerates induced by differential settling. However, based on our experimental setup - which was primarily designed to assess the differences in removal efficiencies

as a function of probe MPs properties – we cannot rule out, that a fraction of the MPs that were removed during the sedimentation phase were dragged along (co-sedimented) with the sludge flocs without interacting with the flocs. However, the low (absolute) zeta potential that we determined for the MPs in filtered wastewater matrix, ruled out repulsive (electrostatic) forces and, thus, only attractive (e.g., van der Waals) forces remained. We, therefore, speculate that the contact between probe MPs and sludge flocs (caused by differential settling) also resulted in the formation of heteroagglomerates. After reaching steady state conditions, about 15 % of the probe PE 60 μm MPs remained in the supernatant and therefore, an additional 10 % of them were removed due to the formation of shear induced heteroagglomeration. Therefore, 85 % of the probe PE 60 μm MPs were heteroagglomerated with sludge flocs. Similar removal fractions can also be anticipated for the probe PE 24 μm MPs, although blank experiments are not available for these particles.

The above considerations are difficult to directly transfer to the probe PVC 40 μm MPs and the probe PS 100 μm MPs due to the (effective) density of the respective MPs. Assuming a density of 1.2–1.4 g cm^{-3} for PVC and 1.05 g cm^{-3} for PS, all these probe MPs should have been removed by gravitational settling in experiments conducted in DI water assuming Stokes' law (see SI Section 10). The effective density of the MPs, however, may have differed from the theoretical values for various reasons (e.g., gas bubbles attached to rough surfaces) as discussed in Section 3.2.2. Therefore, 70 % and 55 % of the probe PVC 40 μm MPs and of the probe PS 100 μm MPs were found in the upper layer in the experiments conducted in DI water. At the timepoint t_0 in kinetic removal experiments, the fraction of the respective probe MPs decreased to 15 % and after reaching steady state conditions the fraction in the supernatant decreased further to 5 % for both MP types. Assuming that the results from blank experiments and from experiments conducted in activated sludge matrix are independent and additive, it can be argued that of the 70 % and 55 % of probe PVC 40 μm MPs and of the probe PS 100 μm MPs, respectively, remaining in the upper layer after the DI experiments, 80 % and 75 % were removed due to heteroagglomeration caused by differential settling. This resulted in the observed 15 % of the respective probe MPs found in the supernatant at timepoint t_0 in the kinetic removal experiments (Table S8). Although the estimated fractions of MPs removed by differential settling for the probe PVC 40 μm (80 %) and for probe PS 100 μm (75 %) are in good agreement with the 75 % estimated for the probe PE 60 μm MPs, the above assumptions are difficult to justify, as the probe MPs that gravitationally settled in DI water may also have heteroagglomerated due to differential settling in the presence of sludge flocs. Unfortunately, our blank experiments are unsuitable to quantitatively distinguish between the impact of gravitational settling of probe MPs and settling of probe MPs - floc heteroagglomerates formed by differential settling. Despite these uncertainties, our experimental results on removed probe MPs fractions (Table S8) combined with the low zeta potential determined for the probe MPs in filtered wastewater matrix, suggest that the formation of heteroagglomerates followed by their sedimentation dominated the removal of MPs during the activated sludge process. This is, furthermore, in qualitative agreement with sludge flocs imaged at the end of the experiments (Figs. S9-S12), showing probe MPs almost exclusively associated with the sludge and only rarely in the liquid phase.

3.4. Relative affinity of probe microplastic particles to sludge flocs

We used the results from the kinetic (time resolved) experiments to estimate the relative affinities of the probe MPs to the sludge flocs. This relative affinity corresponds to the product of $\alpha\beta(n_0,B)B$ (simplified as $\alpha\beta B$ in the following text), where α is the attachment efficiency of MPs to the sludge flocs, B is the concentration of sludge flocs, approximated using the TSS concentration of the activated sludge, and $\beta(n_0, B)$ is the collision frequency which depends on the initial number of probe MPs (n_0) and on B. The relative affinity can be estimated based on the number of probe MPs that were quantified in the supernatant n_{sup} after increasing aeration and mixing time and maintaining the same sedimentation time of 30 min, relative to the total amount of probe MPs added to the system (n_0), using the following equation:

$$\ln\left(\frac{n_0}{n_{sup}}\right) = \alpha\beta(n_0,B)Bt \quad (1)$$

At the beginning of the experiment, the formation of heteroagglomerates is more important than their breakup. This results in a linear relationship between $\ln\left(\frac{n_0}{n_{sup}}\right)$ and mixing and aeration time t, with the slope corresponding to the relative affinity of the probe MPs to the sludge flocs [46,6].

The initial increase of $\ln\left(\frac{n_0}{n_{sup}}\right)$ against time from 0 to 5 min can be described with a straight line for all pristine MPs smaller than 100 μm and for UV-light irradiated PE and PVC (Fig. 7A-C and E-G), reflecting the increasing formation of heteroagglomerates during the first 5 min. For UV light irradiated PS probe MPs (Fig. 7B and F), the kinetics were too fast to be resolved using our experimental approach, and steady state conditions seemed to have established already after minimal mixing times (caused by sample handling), followed by 30 min of sedimentation (see Section 3.3.3). In both kinetic experiments conducted with larger probe MPs, buoyancy (PE: 580 μm) and fast sedimentation (PS: 460 μm) hampered a kinetic analysis of the experimental results (Fig. 7D and H).

With the exception of UV-light irradiated probe PS 100 μm MPs and the larger probe PS 460 μm and PE 580 μm MPs, the slopes indicated in Table 2, corresponding to the relative affinity of the probe MPs to the sludge flocs ($\alpha\beta B$), were within a factor of 2.5 for all MP types between 6 and 100 μm. When correcting for the different TSS contents of the activated sludge (B) from the different experiments, the product of ($\alpha\beta$) remained within a factor of 4 for all MP types (Table 2). It is interesting to note that $\alpha\beta$ calculated for 6 μm PS is considerably lower than $\alpha\beta$ calculated for the other MPs. This size effect can be explained by the reduced collision frequency β, which at these sizes is dominated by the contribution of fluid shear and differential settling [17]. Since Brownian motion is negligible for particles larger than a few microns such as the probe MPs used in our experiments, β is expected to correlate with the size of the particles. Note that the reduced collision efficiency β only slowed down the heteroagglomeration process but did not affect the steady state condition, which is key to the MPs removal.

These results suggest that for the spiked probe MPs of sizes smaller or equal to 100 μm, the agglomeration behavior was largely independent of the polymer type, shape, size and only showed a difference for the UV light irradiated probe PS 100 μm MPs. However, despite the difficulties in assessing the relative affinity of UV-light irradiated PS to sludge flocs, the UV light irradiation rather accelerated the transfer of MPs to the sludge than slowing it down. In contrast, large MPs (~500 μm) transfer to sludge depended on the probe MPs density, with higher density MPs being removed more efficiently than those with lower density.

3.5. Efficient transfer of microplastic particle to the sludge matrix

The formation of heteroagglomerates between sludge flocs and all types of probe MPs investigated in this study reached steady state conditions within 15 mins of mixing and aerations followed by 30 mins of sedimentation. The formation of heteroagglomerates resulted in an efficient transfer of the probe MPs to the sludge. The time needed to establish a steady-state is considerably shorter than the hydraulic retention times in activated sludge systems of full-scale WWTPs [44], underlining the high efficiency of the activated sludge process to transfer MPs from wastewater to sludge. The accumulation of MPs in sedimented sludge is consistent with the efficient removal of MPs in full-scale WWTPs employing activated sludge systems [12,22,31,32,36,4,42]. It

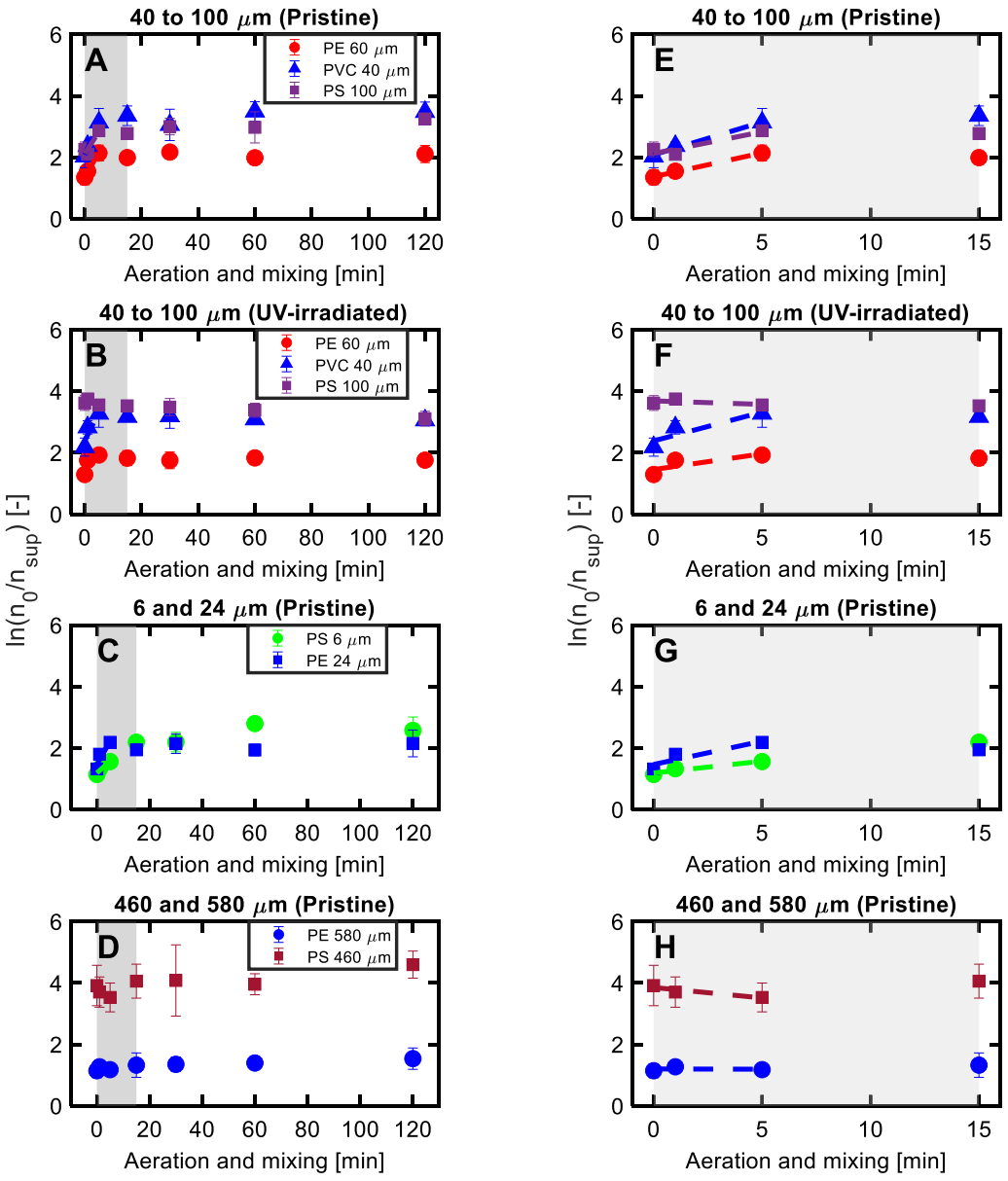

Fig. 7. Natural logarithm of the ratio of the number of probe microplastic particles (MPs, polyethylene (PE),) polystyrene (PS), polyvinyl chloride (PVC) added (n_0) to the number of probe MPs quantified in the supernatant (n_{sup}) as a function of aeration and mixing times for (A, B) pristine probe MPs (40 to 100 μm) and (C, D) UV light irradiated probe MPs (40 to 100 μm), (C, G) pristine probe MPs (6 and 24 μm), and (D, F) pristine probe MPs (460 and 580 μm). Panels E, F, G, and H are enlargements of the areas highlighted in grey in panels A-D, respectively. Note that all experiments included a 30 min sedimentation step conducted after the indicated mixing and aeration times. Error bars correspond to one standard deviation (n = 3). The dashed lines represent linear models fitted to the data collected for aeration and mixing times up to 5 min.

Table 2
Parameters (slope (αβB) and R^2) corresponding to the linear fits of the data shown in Fig. 7. αβ was derived by normalizing the slopes (αβB) to the sludge concentration (B) of the respective experiments. α: sticking coefficient, β: collision frequency, TSS: Total suspended solids.

	PVC 40 μm Pristine	PE 60 μm Pristine	PS 100 μm Pristine	PVC 40 μm UV-irradiated	PE 60 μm UV-irradiated	PS 100 μm UV-irradiated	PS 6 μm Pristine*	PE 24 μm Pristine*	PS 460 μm Pristine	PE 580 μm Pristine
α·β·B [-]	0.21	0.15	0.14	0.19	0.10	n.a.	0.08	0.15	n.a.	n.a.
α·β [L g^{-1}]	0.12	0.09	0.08	0.12	0.07	n.a.	0.03	0.05	n.a.	n.a.
R^2	0.99	1.00	0.85	0.82	0.69	-	0.93	0.85	-	-
Sludge concentration (B) [gTSS L^{-1}]	1.71			1.53			2.97		1.58	

n.a.: not applicable as no kinetic analysis could be performed on the data.
* Values of α·β(n_0, B)·B have to be interpreted with care as the initial number of probe microplastic particles (n_0) and the sludge concentration (B) differed from the other experiments.

is worth noting that due to analytical challenges, reported removal efficiencies are currently limited to MPs > 20 μm. However, our results predict the same removal efficiencies also for MPs down to at least 6 μm.

Before reaching the WWTP, the MPs are transported with the wastewater along the sewer lines. In addition to serving as a conveyor belt, the sewer system also acts as a bioreactor [24] and the MPs likely become coated with organic matter (e.g., proteins and humic acid, so-called eco-corona [30,48]) and possibly a biofilm (e.g., extracellular polymer substances), reducing the hydrophobicity of the (pristine) MPs [45]. As UV-light radiation likely reduced the hydrophobicity of the probe PS 100 μm MPs, and led to an even faster heteroagglomeration of the probe MPs with the sludge flocs, we speculate that the formation of an eco-corona will increase the heteroagglomeration rates. At the concentration of MPs used in this study, and at currently reported MP concentrations in sludge systems, sludge properties are not expected to be affected by the presence of MPs. Nevertheless, several studies investigated the impacts of MPs on activated sludge processes and observed changes in performance of the treatment, such as nitrogen removal [19,47,50]. Although the MP concentrations used in these studies were higher than what is currently reported in the literature, if production volumes of plastics and corresponding amounts of MPs discharged to sewer systems are continuing to increase, a MP induced modification of the floc properties cannot be excluded which may impact heteroagglomeration processes and the respective kinetics.

The estimation of the number of MPs in wastewater systems, and especially the number of MPs discharged into surface waters, is commonly based on quantifying MP contents in WWTP effluent water [31,38,42,8]. This approach has the advantage that the amounts of MPs leaving the WWTP are directly quantified. However, large volumes of (diluted) treated wastewater have to be collected. To accumulate a sufficiently large number of MPs, dead-end filtration is commonly applied resulting in frequent filter clogging that may lead to MPs losses during subsequent filter handling and sample processing. Following our experimental results, indicating that MPs discharged from WWTPs correlate to the TSS in the effluent water, we suggest that discharged amounts of MPs can be estimated based on the MP contents in samples of activated sludge, in combination with routinely monitored total suspended solids (TSS) in the effluent of WWTPs. For PE MPs, our experimental data showed a slightly higher fraction remaining in the supernatants compared to the fraction of TSS remaining in the supernatant. Calculations of discharged amounts of PE MPs based on the PE contents in activated sludge may therefore tend to slightly underestimate PE MPs in the effluent water. It is expected that the degree of underestimation will increase with increasing particle size, as observed for the probe PE 500 μm MPs. Particles of such sizes are, however, rarely observed in WWTP effluents.

Despite these shortcomings, using the MP contents in activated sludge to estimate the amounts of MPs discharged to surface waters offers the following advantages: 1) The higher MP (and TSS) contents in sludge than in the WWTP effluent water allows collecting smaller sample volumes to reach the same MP content. Assuming typical concentrations of 3 g TSS L^{-1} in activated sludge and 10 mg TSS L^{-1} in effluent water, the volume of treated water to be processed would have to be 300 times larger to obtain the same number of MPs associated with the solids. Sampling activated sludge thus greatly reduces sampling efforts. 2) Given continuous stirring of activated sludge, MPs are expected to be more evenly distributed in the activated sludge than in the effluent water. 3) The discharged amounts of MPs from WWTPs over the past decades may also be assessed by investigating biosolids archives as for example conducted by Okoffo et al. [33].

4. Conclusion

Variable physical-chemical properties (e.g., polymer type, size, morphology, and degree of UV-light irradiation) of MPs had only a minor impact on their behavior in batch experiments simulating the activated sludge process. In total, more than 90 % of all spiked MP variants accumulated in the sedimented sludge after 120 min of mixing/aeration followed by 30 min of sedimentation. Most of the spiked MPs (70 – 80 %) were transferred to the sedimented sludge during the 30 min sedimentation. Fluid shear caused by sludge mixing/aeration resulted in the accumulation of additional 15 – 20 % of the spiked MPs in the sedimented sludge. Time resolved experiments (increasing the mixing time from 0 to 120 min followed by 30 min sedimentation) i) revealed similar relative affinities of the MPs to the sludge flocs and ii) demonstrated that steady state conditions, referring to a constant partitioning of the spiked MPs between supernatant and sedimented sludge, were achieved for all MP variants in less than 15 min. Images of sludge flocs collected at the end of the experiments, in combination with almost neutral zeta potentials of the MPs, suggest that the accumulation of the MPs in the sedimented sludge is driven by the formation of heteroagglomerates, likely induced by van der Waals forces. The high degree of MPs removal (70 – 80 %) already observed after 30 min sedimentation without mixing/aeration suggests that heteroagglomerates are dominantly formed by differential setting and fluid shear only plays a minor role.

The efficient and to a large extent non-specific heteroagglomeration of diverse MP types with sludge flocs makes the activated sludge a suitable collector for MPs. This offers the possibility to estimate the amount of MP discharged from WWTP to surface waters based on the MP contents in activated sludge in combination with the total suspended solids in the effluent.

Environmental Implication

During the activated sludge process, different variants of microplastic particles (MPs) are efficiently transferred from wastewater to sludge. The removal is driven by the formation of heteroagglomerates, whereas differential sedimentation is more important than fluid shear. In time resolved experiments (increasing mixing/aeration times followed by 30 min of sedimentation), steady state conditions referring to a constant amount of MPs remaining in the supernatant were achieved in less than 15 min. Activated sludge, thus, serves as a non-specific MP collector allowing to estimate the amount of MPs discharged from wastewater treatment plants based on the MP contents in the sludge.

CRediT authorship contribution statement

Thomas D. Bucheli: Writing – review & editing, Supervision, Methodology, Conceptualization. **Michael Sander:** Writing – review & editing, Supervision, Methodology, Conceptualization. **Mark Wiesner:** Writing – review & editing, Methodology, Formal analysis, Conceptualization. **Guillaume Crosset-Perrotin:** Writing – review & editing, Writing – original draft, Visualization, Methodology, Investigation, Formal analysis, Conceptualization. **Ralf Kaegi:** Writing – review & editing, Supervision, Project administration, Methodology, Funding acquisition, Conceptualization. **Eberhard Morgenroth:** Writing – review & editing, Supervision, Methodology, Conceptualization.

Declaration of Competing Interest

The authors declare the following financial interests/personal relationships which may be considered as potential competing interests: Guillaume Crosset-Perrotin reports financial support was provided by Federal Office for the Environment. If there are other authors, they declare that they have no known competing financial interests or personal relationships that could have appeared to influence the work reported in this paper.

Acknowledgements

The authors would like to thank Matthias Philipp and Brian Sinnet

for the support in the laboratory, and Narain Ashta and Livia Britschgi for reviewing the manuscript. We thank Christoph Hueglin for valuable discussions about and suggestions for the project. Guillaume Crosset-Perrotin and Ralf Kaegi thank the Swiss Federal Office for the Environment for the funding (Grant number: 20.0093.PJ / C3DDE1CBA).

Appendix A. Supporting information

Supplementary data associated with this article can be found in the online version at doi:10.1016/j.jhazmat.2025.139875.

Data availability

Data will be made available on request.

References

[1] Abi Farraj, S., Lapointe, M., Kurusu, R.S., Liu, Z., Barbeau, B., Tufenkji, N., 2024. Targeting nanoplastic and microplastic removal in treated wastewater with a simple indicator. Nat Water. https://doi.org/10.1038/s44221-023-00177-3.
[2] Al Harraq, A., Bharti, B., 2022. Microplastics through the lens of colloid science. ACS Environ Au 2 (1), 3–10. https://doi.org/10.1021/acsenvironau.1c00016.
[3] Al Harraq, A., Brahana, P.J., Arcemont, O., Zhang, D., Valsaraj, K.T., Bharti, B., 2022. Effects of weathering on microplastic dispersibility and pollutant uptake capacity. ACS Environ Au 2 (6), 549–555. https://doi.org/10.1021/acsenvironau.2c00036.
[4] Ali, I., Ding, T., Peng, C., Naz, I., Sun, H., Li, J., Liu, J., 2021. Micro- and nanoplastics in wastewater treatment plants: occurrence, removal, fate, impacts and remediation technologies – a critical review. Chem Eng J 423, 130205. https://doi.org/10.1016/j.cej.2021.130205.
[5] American Public Health Association, 2025. American water works association, & water environment federation. Standard Methods for the Examination of Water and Wastewater, 24th ed.). APHA Press.
[6] Barton, L.E., Therezien, M., Auffan, M., Bottero, J.-Y., Wiesner, M.R., 2014. Theory and methodology for determining nanoparticle affinity for heteroaggregation in environmental matrices using batch measurements. Environ Eng Sci 31 (7), 421–427. https://doi.org/10.1089/ees.2013.0472.
[7] Belone, M.C.L., Yli-Rantala, E., Sarlin, E., Kokko, M., 2025. Microplastics in an anaerobic digester treating sewage sludge: occurrence and factors affecting their identification with Raman spectroscopy. J Hazard Mater, 138015. https://doi.org/10.1016/j.jhazmat.2025.138015.
[8] Ben-David, E.A., Habibi, M., Haddad, E., Hasanin, M., Angel, D.L., Booth, A.M., Sabbah, I., 2021. Microplastic distributions in a domestic wastewater treatment plant: removal efficiency, seasonal variation and influence of sampling technique. Sci Total Environ 752, 141880. https://doi.org/10.1016/j.scitotenv.2020.141880.
[9] Binda, G., Zanetti, G., Bellasi, A., Spanu, D., Boldrocchi, G., Bettinetti, R., Pozzi, A., Nizzetto, L., 2023. Physicochemical and biological ageing processes of (micro) plastics in the environment: a multi-tiered study on polyethylene. Environ Sci Pollut Res 30 (3), 6298–6312. https://doi.org/10.1007/s11356-022-22599-4.
[10] Carr, S.A., Liu, J., Tesoro, A.G., 2016. Transport and fate of microplastic particles in wastewater treatment plants. Water Res 91, 174–182. https://doi.org/10.1016/j.watres.2016.01.002.
[11] Casella, C., Sol, D., Laca, A., Díaz, M., 2025. Microplastic retention in secondary sewage sludge: characterization and influence of solid concentration. Appl Sci 15 (7), 3557. https://doi.org/10.3390/app15073557.
[12] Chand, R., Iordachescu, L., Bäckbom, F., Andreasson, A., Bertholds, C., Pollack, E., Molazadeh, M., Lorenz, C., Nielsen, A.H., Vollertsen, J., 2024. Treating wastewater for microplastics to a level on par with nearby marine waters. Water Res 256, 121647. https://doi.org/10.1016/j.watres.2024.121647.
[13] Chubarenko, I., Bocherikova, I., Esiukova, E., Isachenko, I., Kupriyanova, A., Lobchuk, O., Fetisov, S., 2023. Microplastics in sea ice: a fingerprint of bubble flotation. Sci Total Environ 892, 164611. https://doi.org/10.1016/j.scitotenv.2023.164611.
[14] Frehland, S., Kaegi, R., Hufenus, R., Mitrano, D.M., 2020. Long-term assessment of nanoplastic particle and microplastic fiber flux through a pilot wastewater treatment plant using metal-doped plastics. Water Res 182, 115860. https://doi.org/10.1016/j.watres.2020.115860.
[15] Garnai Hirsch, S., Barel, B., Segal, E., 2019. Characterization of surface phenomena: probing early stage degradation of low-density polyethylene films. Polym Eng Sci 59 (S1), E129–E137. https://doi.org/10.1002/pen.24886.
[16] Gewert, B., Plassmann, M., M, MacLeod, M., 2015. Pathways for degradation of plastic polymers floating in the marine environment. Environmental Science Processes Impacts 17 (9), 1513–1521. https://doi.org/10.1039/C5EM00207A.
[17] Gregory, J., 2006. Particles in water: properties and processes. Part Water.
[18] Gujer, W., 2007. Siedlungswasserwirtschaft, 3rd ed. Springer. https://doi.org/10.1007/978-3-540-34330-1.
[19] Guo, X., Ma, X., Niu, X., Li, Z., Wang, Q., Ma, Y., Cai, S., Li, P., Li, H., 2024. The impacts of biodegradable and non-biodegradable microplastic on the performance and microbial community characterization of aerobic granular sludge. Front Microbiol 15, 1389046. https://doi.org/10.3389/fmicb.2024.1389046.
[20] Hagelskjær, O., Crézé, A., Le Roux, G., Sonke, J.E., 2023. Investigating the correlation between morphological features of microplastics (5–500 μm) and their analytical recovery. Micro Nanoplastics 3 (1), 22. https://doi.org/10.1186/s43591-023-00071-5.
[21] Hartmann, N.B., Hüffer, T., Thompson, R.C., Hassellöv, M., Verschoor, A., Daugaard, A.E., Rist, S., Karlsson, T., Brennholt, N., Cole, M., Herrling, M.P., Hess, M.C., Ivleva, N.P., Lusher, A.L., Wagner, M., 2019. Are we speaking the same language? Recommendations for a definition and categorization framework for plastic debris. Environ Sci Technol 53 (3), 1039–1047. https://doi.org/10.1021/acs.est.8b05297.
[22] Horton, A.A., Cross, R.K., Read, D.S., Jürgens, M.D., Ball, H.L., Svendsen, C., Vollertsen, J., Johnson, A.C., 2021. Semi-automated analysis of microplastics in complex wastewater samples. Environ Pollut 268, 115841. https://doi.org/10.1016/j.envpol.2020.115841.
[23] Horton, A.A., Walton, A., Spurgeon, D.J., Lahive, E., Svendsen, C., 2017. Microplastics in freshwater and terrestrial environments: evaluating the current understanding to identify the knowledge gaps and future research priorities. Sci Total Environ 586, 127–141. https://doi.org/10.1016/j.scitotenv.2017.01.190.
[24] Hvitved-Jacobsen, T., Vollertsen, J., Matos, J.S., 2002. The sewer as a bioreactor – a dry weather approach. Water Sci Technol 45 (3), 11–24. https://doi.org/10.2166/wst.2002.0044.
[25] Kaegi, R., Voegelin, A., Ort, C., Sinnet, B., Thalmann, B., Krismer, J., Hagendorfer, H., Elumelu, M., Mueller, E., 2013. Fate and transformation of silver nanoparticles in urban wastewater systems. Water Res 47 (12), 3866–3877. https://doi.org/10.1016/j.watres.2012.11.060.
[26] Kaegi, R., Voegelin, A., Sinnet, B., Zuleeg, S., Hagendorfer, H., Burkhardt, M., Siegrist, H., 2011. Behavior of metallic silver nanoparticles in a pilot wastewater treatment plant. Environ Sci Technol 45 (9), 3902–3908. https://doi.org/10.1021/es1041892.
[27] Klemmensen, N.D.R., Chand, R., Blanco, M.S., Vollertsen, J., 2024. Microplastic abundance in sludge-treated fields: variance and estimated half-life. Sci Total Environ 922, 171394. https://doi.org/10.1016/j.scitotenv.2024.171394.
[28] Koelmans, A.A., Mohamed Nor, N.H., Hermsen, E., Kooi, M., Mintenig, S.M., De France, J., 2019. Microplastics in freshwaters and drinking water: critical review and assessment of data quality. Water Res 155, 410–422. https://doi.org/10.1016/j.watres.2019.02.054.
[29] MacLeod, M., Arp, H.P.H., Tekman, M.B., Jahnke, A., 2021. The global threat from plastic pollution. Science 373 (6550), 61–65. https://doi.org/10.1126/science.abg5433.
[30] McColley, C.J., Nason, J.A., 2024. Eco-Corona formation on photooxidized plastics exposed to mixed organic matter. Environ Eng Sci 41 (11), 448–458. https://doi.org/10.1089/ees.2024.0103.
[31] Mintenig, S.M., Int-Veen, I., Löder, M.G.J., Primpke, S., Gerdts, G., 2017. Identification of microplastic in effluents of waste water treatment plants using focal plane array-based micro-Fourier-transform infrared imaging. Water Res 108, 365–372. https://doi.org/10.1016/j.watres.2016.11.015.
[32] Murphy, F., Ewins, C., Carbonnier, F., Quinn, B., 2016. Wastewater treatment works (WwTW) as a source of microplastics in the aquatic environment. Environ Sci Technol 50 (11), 5800–5808. https://doi.org/10.1021/acs.est.5b05416.
[33] Okoffo, E.D., Tscharke, B.J., Thomas, K.V., 2023. Predicted growth in plastics entering biosolids and agricultural lands exceeds efforts to control source emissions. ACS EST Water. https://doi.org/10.1021/acsestwater.3c00037.
[34] Petersen, F., Hubbart, J.A., 2021. The occurrence and transport of microplastics: the state of the science. Sci Total Environ 758, 143936. https://doi.org/10.1016/j.scitotenv.2020.143936.
[35] Philipp, M., Bucheli, T.D., Kaegi, R., 2022. The use of surrogate standards as a QA/QC tool for routine analysis of microplastics in sewage sludge. Sci Total Environ 835, 155485. https://doi.org/10.1016/j.scitotenv.2022.155485.
[36] Rasmussen, L.A., Iordachescu, L., Tumlin, S., Vollertsen, J., 2021. A complete mass balance for plastics in a wastewater treatment plant-Macroplastics contributes more than microplastics. Water Res 201 (May), 117307. https://doi.org/10.1016/j.watres.2021.117307.
[37] Rochman, C.M., Hoellein, T., 2020. The global odyssey of plastic pollution. Science 368 (6496), 1184–1185. https://doi.org/10.1126/science.abc4428.
[38] Roscher, L., Halbach, M., Nguyen, M.T., Hebeler, M., Luschtinetz, F., Scholz-Böttcher, B.M., Primpke, S., Gerdts, G., 2022. Microplastics in two German wastewater treatment plants: Year-long effluent analysis with FTIR and Py-GC/MS. Sci Total Environ 817. https://doi.org/10.1016/j.scitotenv.2021.152619.
[39] Rouillon, C., Bussiere, P.-O., Desnoux, E., Collin, S., Vial, C., Therias, S., Gardette, J.-L., 2016. Is carbonyl index a quantitative probe to monitor polypropylene photodegradation? Polym Degrad Stab 128, 200–208. https://doi.org/10.1016/j.polymdegradstab.2015.12.011.
[40] Schefer, R.B., Armanious, A., Mitrano, D.M., 2023. Eco-Corona formation on plastics: adsorption of dissolved organic matter to pristine and photochemically weathered polymer surfaces. Environ Sci Technol. https://doi.org/10.1021/acs.est.3c04180.
[41] Simon, M., van Alst, N., Vollertsen, J., 2018. Quantification of microplastic mass and removal rates at wastewater treatment plants applying focal plane array (FPA)-based Fourier transform infrared (FT-IR) imaging. Water Res 142, 1–9. https://doi.org/10.1016/j.watres.2018.05.019.
[42] Sun, J., Dai, X., Wang, Q., van Loosdrecht, M.C.M., Ni, B.-J., 2019. Microplastics in wastewater treatment plants: detection, occurrence and removal. Water Res 152, 21–37. https://doi.org/10.1016/j.watres.2018.12.050.
[43] Tagg, A.S., Brandes, E., Fischer, F., Fischer, D., Brandt, J., Labrenz, M., 2022. Agricultural application of microplastic-rich sewage sludge leads to further

uncontrolled contamination. Sci Total Environ 806, 150611. https://doi.org/10.1016/j.scitotenv.2021.150611.

[44] Tchobanoglous, G., Stensel, D.H., Tsuchihashi, R., Burton, F., Abu-Orf, M., Bowden, G., Pfrang, W., Metcalf & Eddy, Inc, & AECOM (Eds.). (2014). *Wastewater engineering: Treatment and resource recovery* (Fifth edition). McGraw-Hill Education.

[45] Tu, C., Chen, T., Zhou, Q., Liu, Y., Wei, J., Waniek, J.J., Luo, Y., 2020. Biofilm formation and its influences on the properties of microplastics as affected by exposure time and depth in the seawater. Sci Total Environ 734, 139237. https://doi.org/10.1016/j.scitotenv.2020.139237.

[46] Turner, A.A., Rogers, N.M.K., Geitner, N.K., Wiesner, M.R., 2020. Nanoparticle affinity for natural soils: a functional assay for determining particle attachment efficiency in complex systems. Environmental Science Nano 7 (6), 1719–1729. https://doi.org/10.1039/D0EN00019A.

[47] Wei, W., Huang, Q.-S., Sun, J., Wang, J.-Y., Wu, S.-L., Ni, B.-J., 2019. Polyvinyl Chloride Microplastics Affect Methane Production from the Anaerobic Digestion of Waste Activated Sludge through Leaching Toxic Bisphenol-A. Environ Sci Technol 53 (5), 2509–2517. https://doi.org/10.1021/acs.est.8b07069.

[48] Wheeler, K.E., Chetwynd, A.J., Fahy, K.M., Hong, B.S., Tochihuitl, J.A., Foster, L. A., Lynch, I., 2021. Environmental dimensions of the protein corona. Nat Nanotechnol 16 (6), 617–629. https://doi.org/10.1038/s41565-021-00924-1.

[49] Xu, Y., Ou, Q., Wang, X., Hou, F., Li, P., van der Hoek, J.P., Liu, G., 2023. Assessing the mass concentration of microplastics and nanoplastics in wastewater treatment plants by pyrolysis gas Chromatography–Mass spectrometry. Environ Sci Technol. https://doi.org/10.1021/acs.est.2c07810.

[50] Zhou, C., Wu, J., Ma, W., Liu, B., Xing, D., Yang, S., Cao, G., 2022. Responses of nitrogen removal under microplastics versus nanoplastics stress in SBR: Toxicity, microbial community and functional genes. J Hazard Mater 432, 128715. https://doi.org/10.1016/j.jhazmat.2022.128715.